Optics Communications 407 (2018) 280–284

Contents lists available at ScienceDirect

Optics Communications

journal homepage: www.elsevier.com/locate/optcom

# Bi-dimensional empirical mode decomposition based fringe-like pattern suppression in polarization interference imaging spectrometer

Wenyi Ren [a], Qizhi Cao [b], Dan Wu [c], Jiangang Jiang [a,*], Guoan Yang [d], Yingge Xie [a], Guodong Wang [a], Sheqi Zhang [a]

[a] School of Science, Northwest A&F University, Yangling 712100, China
[b] Key Lab. of Environment Change and Resources Use in Beibu Gulf, MOE, Guangxi Teachers Education University, Nanning 530001, China
[c] College of Mechanical and Electronic Engineering, Northwest A&F University, Yangling 712100, China
[d] School of Electronic and Information Engineering, Xi'an Jiaotong University, Xi'an 710049, China

ARTICLE INFO

*Keywords:*
Fringe analysis
Fourier transform spectrometer
Empirical mode decomposition

ABSTRACT

Many observers using interference imaging spectrometer were plagued by the fringe-like pattern(FP) that occurs for optical wavelengths in red and near-infrared region. It brings us more difficulties in the data processing such as the spectrum calibration, information retrieval, and so on. An adaptive method based on the bi-dimensional empirical mode decomposition was developed to suppress the nonlinear FP in polarization interference imaging spectrometer. The FP and corrected interferogram were separated effectively. Meanwhile, the stripes introduced by CCD mosaic was suppressed. The nonlinear interferogram background removal and the spectrum distortion correction were implemented as well. It provides us an alternative method to adaptively suppress the nonlinear FP without prior experimental data and knowledge. This approach potentially is a powerful tool in the fields of Fourier transform spectroscopy, holographic imaging, optical measurement based on moire fringe, etc.



## 1. Introduction

Fringe-like pattern (FP) in CCD images occurs due to an interference effect similar to Newton Rings. The production of constructive and destructive interference patterns can cause substantial quantum efficiency variations in back-thinned CCDs as long wavelength light is multiply reflected between the front and back surfaces. FP begins to be an important issue for CCDs when the absorption depth within the silicon becomes comparable to the thickness of the CCD. This occurs for optical wavelengths in red and near-infrared (NIR) region. The light is internally reflected several times before finally being absorbed [1,2]. If the FP is not corrected, it can adversely affect the science derived from the data.

There were many methods proposed to suppress the FP. The approach for the fringe removal option within the widely used *ccdproc* task in IRAF, but this method can considerably over- or under-correct due to the intrinsic variations of the night sky-emission lines, which are not correlated to exposure time [3]. The *ccdproc* task also gives the option of specifying additional scaling factors via image headers, but this requires considerable manual iteration to get a satisfactory result. Howell has proposed a method which uses a neon lamp as a flat field source and produces high signal to noise ratio(SNR) fringe frames to use for defringing an image during the calibration process [4]. An empirical method for the removal of the FP in the spectral domain and the intensity variations in the imaging domain was proposed by Lagerholm to improve the derived results from VIMOS-IFU data [5,6]. However, the empirical method was constructed and tested on data with slowly varying spectral properties. For other types of data, such as with strongly varying background or low intensities (the FP scales with the intensity), a different approach should be preferred. In these cases it may be better to rely on the combination of several exposures thus mimicking the averaging effect. An automatic fringe removal method to the EFOSC images was proposed by Colin [7]. However, the knowledge of the pattern is an essential part of the method. That is, it is not adaptive. In this paper, an adaptive FP suppression method based on bi-dimensional empirical mode decomposition (BEMD) was proposed for the preprocessing of raw data taken by the polarization interference imaging spectrometer (PIIS) [8,9].

* Corresponding author.
*E-mail address:* renovel@nwsuaf.edu.cn (J. Jiang).

https://doi.org/10.1016/j.optcom.2017.09.071
Received 28 April 2017; Received in revised form 20 September 2017; Accepted 21 September 2017
Available online 2 October 2017
0030-4018/

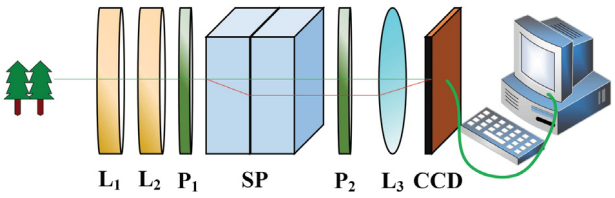


**Fig. 1.** The schematic of PIIS.

## 2. Polarization interference imaging spectrometer

PIIS is an imaging spectrometer proposed by Zhang to acquire the spatial and spectral information of the target simultaneously [10,11]. As shown in Fig. 1, the collimating lens is composed by the lenses $L_1$ and $L_2$; $P_1$ is the polarizer; the Savart polariscope, $SP$, is used as a beamsplitter to split the incident into two rays whose polarization orientation are perpendicular to each other; $P_2$ is the analyzer; $L_3$ is the imaging lens; the CCD is placed on the focal plane of $L_3$; the computer is used to storage and process the raw data. The spatial information can be obtained via realigning the data cube. The spectral information should be retrieved from the realigned interferogram data cube by the fast Fourier transform or other approaches. As shown in Fig. 1, a data cube with the spatial and spectral information could be obtained after the data processing. The raw data taken by the PIIS is the superstition of the image and interferogram which can be taken by the traditional camera and Fourier Transform spectrometer, respectively [12,13]. That is, the spatial and spectral information both are coded in the raw data. PIIS is the combination of the traditional camera and Fourier Transform spectrometer.

The specifications of the PIIS are as follow: the wavelength range is from 480 to 960 nm; the band number is 128; the spectral resolution is 81.4 $cm^{-1}$; the CCD is produced by Sarnoff Corporation (CAM512, 512×512 pixels, the pixel size is 18 μm×18 μm).

Calibration is a vital and essential procedure during the data processing and information retrieval. During the wavelength and spectral response calibration, the interferogram generated by the monochromatic source must be generated. A back-thinned Sarnoff CCD array is utilized as a detector. If the wavelength is in the red or NIR region, the interferogram would be contaminated by the FP. Consequently, the precise spectrum would not be obtained after the calibration and information retrieval processing.

## 3. Bi-dimensional empirical mode decomposition

Bi-dimensional empirical mode decomposition (BEMD), a powerful tool for the adaptive and nonlinear image processing, is the extension of empirical mode decomposition (EMD) method proposed by Huang for the nonlinear signal and image processing [14,15]. BEMD has been successfully utilized in pattern recognition, image de-noising, image enhancement, image fusion, etc. [16,17]. In this paper, the raw contaminated images taken by PIIS were decomposed into different intrinsic mode functions (IMFs) which are corresponding to certain content of the image. The sifting procedure of BEMD is implemented by the following steps:

Step 1. Find out all the local maximal and minimal points of the image, respectively;

Step 2. Create the upper and lower envelopes by the spline interpolation of the local maximal and minimal, respectively;

Step 3. For each time, take the mean of the upper and lower envelopes;

Step 4. Subtract the mean image from input image;

Step 5. Check whether the average value of mean image is close enough to zero. If not, repeat the process from step 1 with the result image from step 4 as input image. If it is, the result is IMF, define the residue as result from IMF subtracted from input image;

Step 6. Find out the next IMF by starting over from step 1 with the residue as a new input signal.

## 4. Fringe-like pattern suppression based on BEMD

According to BEMD, an image $I(x, y)$ can be decomposed into $N$ IMFs and the residue $r(x, y)$ as

$$I(x, y) = \Sigma_{k=1}^{N} IMF_k(x, y) + r(x, y). \quad (1)$$

According to EMD and the properties of the interferogram and FP, we can obtain that:

(1) The frequency of $IMF_k(x, y)$ decreases with its order index $k$ [15];

(2) The monochromatic interferogram is corresponding to the high frequency component of image $I(x, y)$ [18,19];

(3) The FP, which is determined by the structure of CCD, is stable with time and corresponding to the low frequency component of $I(x, y)$ [17–19].

Thereby, the FP, $F(x, y)$, can be reconstructed as

$$F(x, y) = \Sigma_{k=\kappa+1}^{N} IMF_k(x, y) + r(x, y). \quad (2)$$

The reconstructed interferogram, $I_{Rec}(x, y)$, is given by

$$I_{Rec}(x, y) = \Sigma_{k=1}^{\kappa} IMF_k(x, y). \quad (3)$$

The threshold index, $\kappa$, is obtained by

$$\Gamma_\kappa \geq \Gamma_{\kappa+1}, \quad (4)$$

where $\Gamma_i = \frac{H(I_{Rec}(x,y))}{H(F(x,y))}$; $H(\cdot)$ is the image information entropy; $I_{Rec}(x, y)$ and $F(x, y)$, respectively, are reconstructed by Eqs. (2) and (3) while $\kappa = i$.

## 5. Experiment

The contaminated monochromatic interferogram, generated by the source with wavelength of 880 nm, taken by PIIS is shown in Fig. 2(a). The contaminated polychromatic interferogram, generated by a mixtured source of xenon and halogen lamps, is shown in Fig. 2(b). It is obvious that the interferograms had been dramatically distorted by the FP. As shown in Fig. 3, the interferograms shown in Fig. 2(a) and (b) were decomposed into 5 IMFs and the residual via BEMD, respectively. Fig. 3(a) and (g) are the first BIMFs of the interferograms shown in Fig. 2. Fig. 3(f) and (i) are the residuals of the interferograms shown in Fig. 2. As shown in Fig. 3(a) and (l), it was discovered that there are approximately 5 longitudinal and 1 horizontal stripes which are introduced by the CCD mosaic [20]. CCD mosaic, a solution to get a widen-field using the existing CCDs, is to use multiple CCDs to tile the bigger field of view. Some stripes can be found in the original images taken by the mosaic CCD. For example, it has been reported by many researchers [21,22]. Based on their works, the stripes can be both existed in the systems based on the monochromatic and chromatic CCDs. Furthermore, the mosaic stripes were found both the monochromatic and polychromatic interferogram. It can be observed that the interferogram information mostly is coded in the prior IMFs. The FP mainly is coded in the other IMFs and the residuals.

According to the definition of $\Gamma$ and the decomposition result shown in Fig. 3, the curves of $\Gamma$ varying with index $i$ were obtained and shown in Fig. 4. $\kappa_m$ and $\kappa_p$, respectively, are the threshold indexes with respect to the monochromatic and polychromatic interferograms. It can be obtained that both the two threshold indexes are 1. Thereby, the interferograms and FPs can be reconstructed based on Eqs. (2) and (3). The reconstructed results were shown in Fig. 5(a)–(d). Fig. 5(a) and (c), respectively, are the reconstructed monochromatic and polychromatic